Zebrafish in Research and Education
2019 *Eastern Biologist* Special Issue 1:15–32

Analysis of Genetic Interactions and Developmental Requirements of the β1,3-*N*-acetylglucosaminyltransferase Family During Zebrafish Development

Quentin J. Machingo[1,2,*], Anandita Seth[2,+], Mary Adely[1], Lauren Wagner[1], Andreas Fritz[3], and Barry D. Shur[2]

Abstract - Glycosyltransferases are responsible for the synthesis of complex carbohydrates and are known to be essential for many developmental processes. Furthermore, loss-of-function studies have demonstrated that an individual glycosyltransferase can have a wide range of functions. To better understand the function of glycosyltransferases during embryonic development, a family of β1,3-*N*-acetylglucosaminyltransferases (β3GnT) was identified and assayed for expression and function throughout zebrafish development. We characterized the six members of the β1,3 *N*-acetylglucosaminyltransferase family in zebrafish. Temporal and spatial expression data indicate a diverse expression profile for each family member. Morpholino knockdown of the transcripts revealed a spectrum of phenotypes, all affecting the development of the CNS and the trunk mesenchyme. Specifically, knockdown of β3GnT2a affected hindbrain specification and axial patterning, while knockdown of β3GnT5 disrupted retinal patterning. Simultaneous knockdown of multiple family members revealed synergism and functional redundancy that had not previously been reported *in vivo* during vertebrate development. This report demonstrates that *N*-acetylglucosaminyltransfe rases have essential roles in diverse aspects of embryonic development, including the hindbrain and retinal development. Furthermore, we have uncovered functional synergisms between these glycosyltransferase family members. Continued analysis of these genes will provide additional information into the mechanism by which glycosyltransferases regulate embryonic development.

Introduction

Complex carbohydrate side-chains decorate many extracellular and membrane-bound glycoproteins and glycolipids, and it is becoming evident that they have significant and diverse functions during embryonic development and homeostasis in adults. Gaining insight into the specific function of any particular glycan chain has proven difficult, due partly to the heterogeneity of the glycan chains and partly to the abundance of glycosyltransferases found in vertebrate genomes. Most glycosyltransferases are localized to the endoplasmic reticulum or the Golgi apparatus where they catalyze the addition of monosaccharide residues onto growing carbohydrate chains (Varki 1993). By convention, glycosyltransferases are classified according to the monosaccharide they recognize and the glycosidic linkage they generate; for example, an enzyme that recognizes the monosaccharide *N*-acetylglucosamine (GlcNAc) and generates a β1,3 linkage would be called a β1,3-*N*-acetylglucosaminyltransferase (β3GnT), regardless of the target substrate. Furthermore, while β3GnTs utilize UDP-GlcNAc as their carbohydrate donor, each β3GnT enzyme may be capable of glycosylating different target substrates (Kanie et al. 1993).

The classification of glycosyltransferase genes into biosynthetic families has often been attempted prior to any analysis of the enzymatic function, which has led to mischar-

[1]Department of Biology, Manhattan College, Riverdale, NY 10463. Departments of [2]Cell Biology and [3]Biology, Emory University, Atlanta, GA 30322. [+] Current address: Lonza Houston, Houston, TX 77006. [*]Corresponding author: Quentin J. Machingo, 3825 Corlear Avenue, Room 317B, Riverdale, NY 10467; quentin.machingo@manhattan.edu.

acterization of glycosyltransferase genes in the past. Originally, it was thought that the catalytic activity of an enzyme could be determined by independent analysis of the protein sequence; while this is possible, assigning functionality based on the analysis of a single nucleotide sequence can pose significant challenges, particularly with glycosyltransferase genes. It has been shown that changes to as few as four amino acids in the substrate recognition site can alter the substrate recognition and therefore the catalytic activity of a glycosyltransferase (Yamamoto et al. 1990). Moreover, the classification of β1,3 galactosyltransferase (β3GalT) genes and β3GnT genes has been particularly difficult and has occasionally resulted in the misclassification of β3GnT genes as β3GalT genes (Shiraishi et al. 2001, Zhou et al. 1999).

Despite the difficulties inherent in studying a polymorphic enzyme family, β3GnT genes have been successfully identified and their functions during development assayed. The mammalian β3GnT genes that have been characterized have diverse functions during embryonic development and throughout the life of the organism. Two in particular; Human β3GnT2, which is the predominant poly-*N*-acetyllactosamine synthase and β3GnT5, which in Humans modifies sphingoglycolipids, have been subjected to a range of functional analyses (Togayachi et al. 2010). Traditional knockout of β3GnT2 in mice did not reveal major developmental defects but did show defects in the activation of T-cells (Togayachi et al. 2010). In contrast, a conditional knockout of β3GnT2 in olfactory neurons of mice suggested an involvement in axon guidance of these cells; however a direct mechanism was not identified (Knott et al. 2012). Similarly, knockout of the β3GnT5 gene in mice produced variable results. Biellmann et. al. concluded that β3GnT5 function was essential during preimplantation development, as homozygous null animals were not viable past implantation. However, Kuan et. al. reported that only a portion of expected homozygous null failed to survive gestation, and the resulting mice had defects in B-cell development (Biellmann et al. 2008b, Kuan et al. 2010). Finally, in adult Humans, altered β3GnT activity has been linked to cancer progression and metastasis. Specifically, the activity of β3GnT2 is up-regulated during pancreatic cancer, with β3GnT2 thus acting as an oncogene, while β3GnT1 shows tumor suppression activity during epithelial metastasis (Bao et al. 2009, Hayashi et al. 2004). All of these reports indicate that knockout of specific β3GnTs have pleiotropic and variable effects, suggesting the possibility of redundancy within the β3GnT family.

Another family of glycosyltransferases that has critical functions during development is the *fringe* protein family (*lunatic*, *manic* and *radical* in mammals). All fringe proteins encode glycosyltransferase activity, and *lunatic fringe (lfng),* in particular, has β3GnT activity (Johnston et al. 1997)**.** *Lfng* glycosylates *O*-fucose epitopes present on *Notch* and potentiates the *Notch-Delta* interactions (Rampal et al. 2005). While *Lfng* is essential for these specific Notch-Delta interactions, it is possible that other β3GnT genes could partially compensate for the loss of *lfng*, or that β3GnT genes provide other essential functions during embryonic development. Furthermore, while much attention has been given to the function of *N*-acetylglucosaminyltransferases, their products and their target substrates, as well as their role in the initiation and progression of cancer metastasis, a complete analysis of their functions during vertebrate development has yet to be presented.

In this study, we investigate the function of the zebrafish β1,3-*N*-acetylglucosaminyltransferase family during zebrafish embryonic development. Six previously cloned zebrafish genes were characterized as β3GnTs and distinguished from the β3GalT and *fringe* families. The temporal and spatial expression pattern of each β3GnT gene was also determined. The function of each gene during development was assessed by morpholino-mediated knockdown and revealed a spectrum of developmental requirements pertaining

to the patterning of the central nervous system (CNS) as well as in patterning the trunk mesenchyme. Initial analysis of the underlying mechanisms suggests an essential function for β3GnT2a in the development of the hindbrain and for β3GnT5 in the development of the retina. Moreover, co-knockdown of multiple β3GnT family members uncovered evidence for functional synergism and redundancy that has been implied but never demonstrated *in vivo*. These results suggest that the β3GnT family of glycosyltransferases regulate multiple essential developmental pathways pertaining to the CNS and mesenchyme in vertebrates. Furthermore, an appreciation of the synergistic properties of this enzyme family may provide more insight into their developmental functions than the single gene knockouts have provided thus far.

Methods

Zebrafish husbandry

Zebrafish were maintained at 28°C in animal facilities at Emory University and Manhattan College as described previously (Westerfield 2000). The wild-type strains AB or Tü were used for all experiments and produced identical morpholino induced phenotypes. All experiments with zebrafish were conducted following IACUC approved protocols.

Cladogram

Sequences encoding predicted zebrafish β1,3-*N*-acetylglucosaminyltransferases were obtained from the Sanger and NCBI databases. Confirmed mammalian sequences were used for a BLAST search to identify putative zebrafish genes. The identified sequences were compared to other vertebrate β1,3-*N*-acetylglucosaminyltransferases as well as to zebrafish, mouse and human β1,3-galactosyltransferases and *fringe* proteins using Clustal W and MegAlign (DNASTAR) software.

Cloning and RT-PCR

Zebrafish β1,3-*N*-acetylglucosaminyltransferases were cloned from cDNA libraries produced using total RNA isolated from; oocytes, 90% epiboly, 1-somite, 20-somite, 26-somite, and Prim-16 staged embryos using RETROscript (Ambion). The PCR products were cloned into dual promoter pCRII vectors (Invitrogen) and carried in E.coli. For *in situ* hybridizations DIG-labeled RNA was in vitro transcribed using either T7 or Sp6 RNA polymerases and was cleaned using MEGAclear transcriptional clean-up to generate labeled probes.

Real time reverse transcriptase PCR was performed to determine the relative levels of mRNA expression. Total RNA was isolated from; oocytes, 90% epiboly, 20 somite and Prim-16 staged embryos using Tripure (Roche) reagent. After isolation the total RNA was treated with DNase to eliminate any contaminating DNA and cleaned by phenol extraction. The total RNA was used as an input for a one-step real time RT-PCR using the SYBR green Universal Master Mix and Light Cycler systems (BioRad). The expression of all β3GnTs were normalized to the zebrafish housekeeping gene zbrul to evaluate the relative levels of gene expression.

Morpholino and mRNA microinjections

One - two cell staged wild-type embryos were microinjected with 1–10 ng of translation blocking anti-sense morpholino oligonucleotides (GeneTools). For control, an equivalent mass of standard control morpholino oligonucleotides was injected (GeneTools). For a

complete list of morpholino oligonucleotide sequences see Table 1. Mature mRNA encoding zebrafish β3GnTs was transcribed from plasmids containing full coding sequences using mMessage mMachine kit (Ambion). Embryos were injected with varying concentrations of either sense or antisense mature mRNA.

Lectin blots

Embryos injected with either control or β3GnT morpholinos were allowed to develop for 24 hours post injection (hpi). Embryos were then manually dechorionated and the yolks were removed using a needle to puncture the yolk membrane allowing the yolk particles to diffuse away. The isolated embryonic tissue was lysed in 2 ul per embryo of ice-cold lectin extraction buffer (0.15M NaCl, 10 mM EDTA, 20 mM Tris-HCl pH 7.6, 0.5% Triton X-100 w/v). The lysate was sheered with a 27-g needle, and the protein concentration was determined with a Micro BCA protein assay kit (Pierce).

The protein lysates were loaded in equal concentrations and resolved on 6% SDS-PAGE. The gel was transferred to a PVDF membrane and blocked with 1x Carb-Free blocking solution (Vector Labs) for 45 min. at 37ºC. The membrane was blotted with 5 µg/ml LEA-AP (EY Labs) for 2 h at room temperature. LEA reactivity was determined with BCIP/NBT.

***In situ* hybridizations and whole mount lectin staining**

Embryos were staged according to morphology as previously described (Kimmel et al. 1995). All embryos were fixed in 4% paraformaldehyde overnight at 4ºC, for stages later than 24 hours, embryos were grown with 0.003% PTU to prevent melanin synthesis. *In situ* hybridizations were performed as previously described (Thisse and Thisse 1998). Anti-sense probes targeting zebrafish β3GnTs as well as *ptch2*, *pax2.1*, *pax6* and *isl1* were used. *In situ* hybridizations on control and morpholino injected embryos were conducted in parallel where necessary. Control hybridizations were performed using sense probes to establish levels of background.

Embryos were prepared for lectin staining as described above for in situ hybridizations. After fixation in methanol, embryos were rehydrated into PBST (PBS + 0.1% tween-20). Embryos were then incubated in LEA-AP for 12 hours at 4°C. Embryos were then washed in PBST and AP activity was detected using BCIP/NBT.

Histology

Formaldehyde fixed embryos were dehydrated in an ethanol series and embedded in paraffin wax. Ten µm thick sections were cut and fixed onto slides. For staining, the tissue was de-waxed in xylenes, rehydrated and stained with hematoxylin and eosin.

Quantification of eye proportions

Digital images were taken of hematoxylin and eosin stained eyes. For each image centered at the optic nerve, the total depth of the eye was determined from the distal membrane of the lens to the medial membrane of the photoreceptor layer. All measurements were conducted in duplicate following a double blind protocol and two adjacent sections were quantified for each embryo. The proportional contribution of every layer within the eye was calculated

Table 1. Anti-sense morpholino oligonucleotides used in the study.

Target gene	Morpholino sequence 5'–3'
β3GnT2a	GCCATGACCTTCACCTTCCTCCGAG
β3GnT2b	GTTCCAGTTGTTACTCATCTTGAAG
β3GnT3	CCACATTCTTCTTTTTCATCTTGGC
β3GnT5	ATGAACATTCTGTTAAGCCACACGC
β3GnT7a	TGAGCAGAGAGGTAAACTCCATATT

for each measurement and the average proportional contribution of each layer was then calculated for all embryos assayed. Standard error was calculated and a two-tailed equal variance t-test was performed to determine statistical significance.

Results

Zebrafish have six conserved members of the β1,3-*N*-acetylglucosaminyltransferase family

Five genes encoding β3GnTs were previously identified in the zebrafish genome and were designated SSP1 through SSP5 (Chou et al. 2000). Originally, these genes were classified as encoding β1,3-galactosyltransferases based on analysis of the individual nucleotide sequences, which was a realistic conclusion due to significant similarities in catalytic domains. Using more recent molecular phylogenetics and comparing the SSP sequences to other vertebrate β3GnT as well as β3GalT genes, we have determined that the genes originally identified as SSPs most likely encode enzymes with β3GnT activity (zebrafish β3GnT sequences are red in Figure 1). Furthermore, analysis of the molecular phylogeny

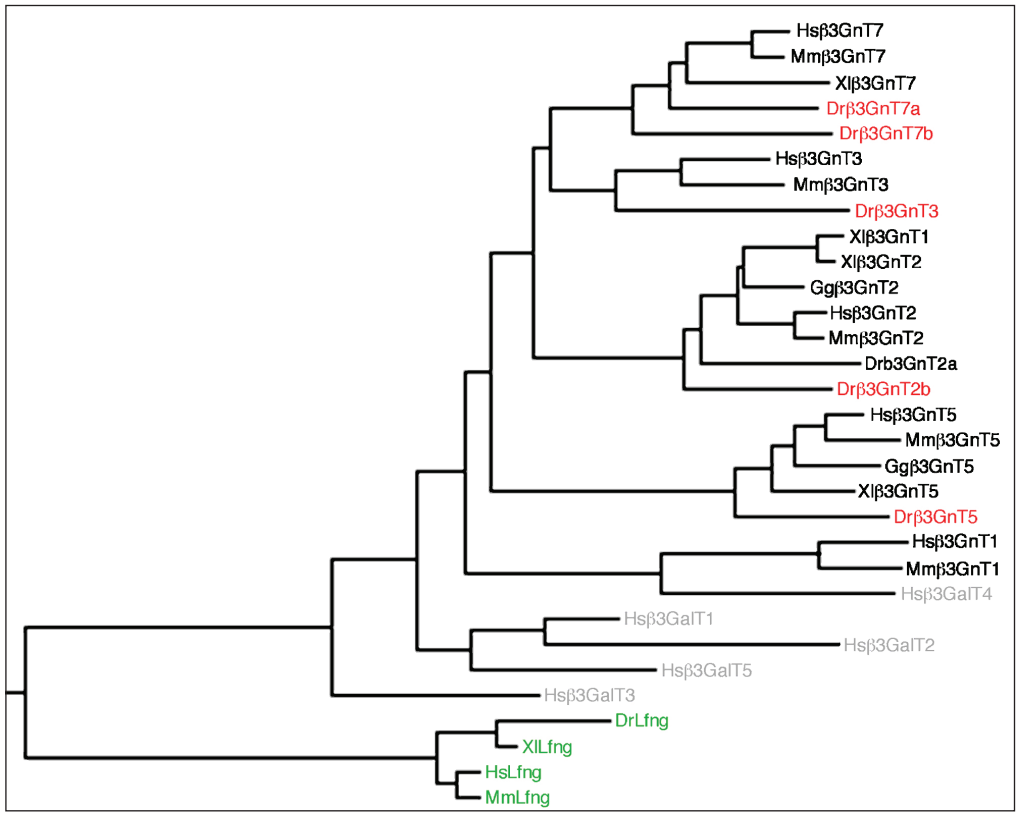

Figure 1. Cladogram of vertebrate β3GnT peptide sequences. Phylogenetic tree showing the relationships of vertebrate β3GnT peptide sequences. Zebrafish (Dr) sequences are in red, Human (Hs), Mouse (Mm), Xenopus (Xl) and Chicken (Gg) are shown for comparison if the orthologous sequence is known. The closely related β3GalT family (grey) partially segregates away from the β3GnT family with the exception of the mammalian β3GnT1s. A clade containing *lunatic fringe* (*Lfng*) sequences, whose proteins have β1,3-*N*-acetylglucosaminyltransferase activity, segregates independently (green). The tree was rooted with zebrafish *GAPDH*.

of various vertebrate β3GnTs and β3GalTs clearly segregates the β3GnT family from the β3GalT family. The β3GnT family can be further divided into clades that selectively group the various members of the family, indicative of the different isoform designations. In cases where more than one orthologous gene grouped into a clade (see β3GnT2s and β3GnT7s in Fig. 1) the "a" designation was assigned to one gene while the more divergent gene of the pair was given the "b" designation.

The one member of the β3GnT family that is present in "higher" vertebrate genomes (rodents and primates) that does not appear in the zebrafish genome is β3GnT1. The only non-mammalian vertebrate species reported to contain a β3GnT1 homolog is *Xenopus laevis*. Our phylogeny places this *Xenopus* orthologue within the β3GnT2 clade, closely grouped with the *Xenopus* β3GnT2 gene (Fig. 1). The phylogenetic relationship of these two genes suggests they may be duplicate genes with neither one being a true β3GnT1 homolog. The mammalian versions of the β3GnT1 gene assort most closely with the β3GalT family, β3GalT4 in particular, rather than with the β3GnT family, and serves to highlight the close evolutionary relationship between the two protein families. We attempted to identify a zebrafish β3GnT1 homolog and located several regions in the zebrafish genome that resemble regions of a β3GnT1 homolog. None of the identified sequences contained a complete reading frame or conserved upstream regulatory elements, suggesting that the zebrafish genome does not contain a functional β3GnT1 gene. We cannot exclude the possibility that the genome contains a highly divergent β3GnT1 gene; moreover, it is possible that the zebrafish genome is continuing to evolve a functional β3GnT1 homolog. This latter idea raises the interesting possibility that β3GnT1 is required for mammalian specific functions. This is supported by a recent report suggesting that β3GnT1 is required for male sexual behavior in mice (Biellmann et al. 2008a). Alternatively, it is possible that there are developmental requirements for β3GnT1 in lower vertebrates that can be compensated for by the other β3GnT enzymes.

Another enzyme that has β3GnT activity and a defined cell signaling function is *lunatic fringe* (*Lfng*). *Lfng* is a classic β3GnT and is a key regulator of the Notch signaling pathway (Dunwoodie 2009). *Lfng* activity is required to attenuate the Notch-Delta interactions, and it appears that Notch is the only endogenous target for *Lfng* (Rampal et al. 2005). Sequence analysis of several *Lfng* genes classifies *Lfng* into a distinct clade, divergent from the β3GnTs and β3GalTs even though *lfng* has β3GnT activity (green in Fig. 1). The divergence may be due to differences in N-terminal residues between the *Lfng* and β3GnT peptides, as the N-terminal residues of classical glycosyltransferases are believed to be regulatory in nature and may also play a role in subcellular localization (Colley 1997). Our phylogenetic analysis of β3GnTs, β3GalTs and *lfng* suggests that substrate specificity/recognition and not catalytic activity may be the primary determinant for phylogenetic relationships within the β3GnT/β3GalT superfamily.

β3GnTs have a diverse and widespread expression pattern throughout development

In order to understand the functional requirement of the zebrafish β3GnTs during embryonic development, we first determined the expression profile of each gene. The temporal expression of the β3GnTs was determined by qRT-PCR using staged total RNA (Fig. 2A). All of the β3GnT genes were expressed to some level at each of the tested stages, although there was noticeable variation between the levels of expression of the six β3GnT genes. β3GnT7a showed the highest level of expression overall at the 90% epiboly stage, while the two β3GnT2 genes; β3GnT2a and β3GnT2b showed the most consistent levels of expression at all stages tested.

To determine where in the embryo each β3GnT gene was expressed, *in situ* hybridizations were performed. To reduce the incidence of overlap with other β3GnT transcripts, *in situ* hybridization probes were designed to the more divergent 5'-ends of each transcript. All β3GnTs showed widespread expression throughout development with limited localized expression. Representative examples of β3GnT2a (B-B"), β3GnT5 (2C-C") and β3GnT7a (2D-D") at the 10 somite stage (B,C,D), 18 somite stage (B', C', D') and at the Prim-6 stage (B', C', D") demonstrate the ubiquitous overlapping expression patterns typically seen with all β3GnT genes. As expected with its consistently high levels of expression, β3GnT2a was detected throughout the embryo at early stages of development (70% epiboly - 48 hpf), although by the 26-somite stage a refined expression was observed in the midbrain/hindbrain boundary (arrowheads in Fig. 2E), the otic vesicle (double arrow in Fig. 2E) and in the pronephros (arrow in Fig. 2E). At the Long-pec stage, β3GnT5 expression was enriched in the developing lens (arrow in Fig. 2F) and ventral midline of the CNS (arrowheads in Fig. 2F). *In situ* hybridizations with sense probes targeting the same transcript showed no reactivity, confirming the specificity of the reported expression.

Knockdown of β3GnTs causes various developmental defects and reveals synergism between β3GnT transcripts

To characterize the function of the β3GnTs during development, gene specific knockdowns were performed using morpholino oligonucleotides (MO). Injection of 10 ng of morpholino targeting a single β3GnT transcript resulted in several distinct phenotypes, however each phenotype showed a consistent theme of affected structures. When we identified a phenotype associated with a given transcript, we titrated the concentration of the morpholino (between 1 ng and 20 ng) to identify the lowest level and highest level that would still produce our reported phenotype. Identifying this range was critical, as when we would inject multiple morpholinos, we needed to use the lowest concentration for each morpholino possible while still keeping the total morpholino below the upper threshold.

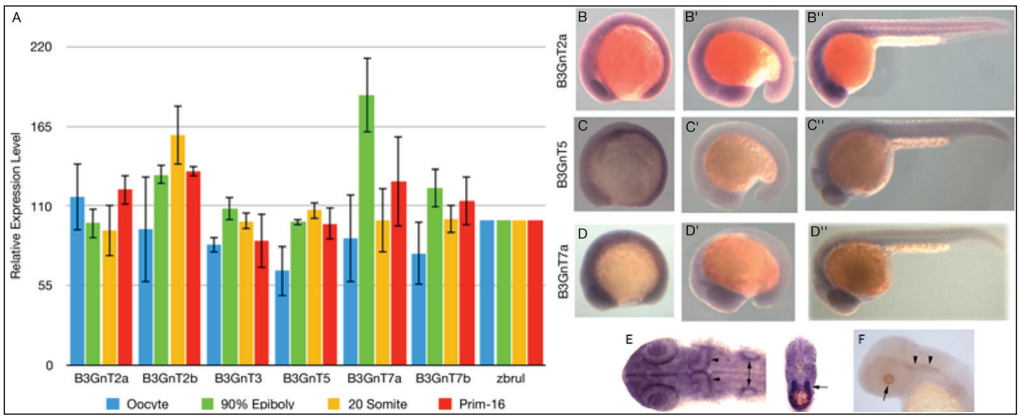

Figure 2. β3GnT family genes have diverse expression profiles. (A) Quantification of RT-PCR from mRNA isolated from oocytes, 90% epiboly, 20-somite, and Prim-16 staged embryos for the six zebrafish β3GnT genes. All values are relative and are normalized to the housekeeping gene zbrul. *In situ* hybridization for β3GnT2a (B-B"), β3GnT5 (C-C") and β3GnT7a (D-D") at 10 somites (B,C,D), 20 somites (B', C', D') and 26 hpf (B", C", D") shows widespread expression though out the embryo. (E) ISH for β3GnT2a with a flat mount or section shows increased expression in the midline of the forebrain and midbrain, at the midbrain/hindbrain boundary (arrowheads), otic vesicles (double arrow), and nephric duct (arrow in cross-section). *In situ* hybridization for β3GnT5 at 72 hpf (F) shows expression localized to the lens (arrow) and at the CNS midline (arrowheads).

We determined that 1.5 ng per morpholino was the lowest level we could use to achieve this goal therefore when morpholinos targeting all family members were injected together, the total morpholino load on an embryo would be 9 ng. For most of our studies we used the higher concentration of 10 ng of each morpholino ensuring a comparable morpholino load throughout the experiment. By using a constant concentration for all transcripts we were able to normalize for effects of morpholino concentration on the phenotype. Typically when we injected higher concentrations of morpholino, the severity of the phenotype increased, but the classification of the phenotype was not altered. In general, knockdown of β3GnT transcripts affected the patterning of the CNS, especially the midbrain/hindbrain region, as well as affecting the development of the trunk. With respect to the trunk, we typically observed either truncations of the tail or disorganization of the tail mesenchyme.

The phenotypes resulting from knockdown of the various β3GnTs were classified based on the degree of the affected phenotype (Fig. 3A-G and summarized in Tables 2, 3, and 4). Class 1 embryos are phenotypically wild-type, whereas Class 2 through Class 8 embryos showed progressively more severe defects in the CNS and trunk, such that Class 8 embryos have the most significant patterning defects throughout the embryo. Control-injected embryos or embryos injected with β3GnT2bMO, β3GnT5MO and β3GnT7bMO all resulted in Class 1 (wild-type) phenotypes at 24 hours post injection (hpi). In contrast, injection of 10 ng of β3GnT2aMO resulted in embryos with an abnormally patterned hindbrain, and globularization of the gut yolk (Fig. 3B) that were classified as Class 2 embryos. Knockdown of β3GnT3 (Fig. 3C) resulted in a more severe phenotype than β3GnT2aMO injected embryos and was classified as Class 3 phenotype. Finally, the injection of β3GnT7aMO produced severely affected embryos with abnormal posterior tail structure and severe patterning defects in the mid and hindbrain (Fig. 3E) that were classified as Class 5 embryos.

The injection of MOs targeting individual β3GnT genes shows that most, if not all, β3GnT genes regulate processes involved in the patterning of the CNS as well as the trunk mesenchyme. Furthermore, the wide array of severity indicates some degree of functional diversity between these genes during zebrafish development. Moreover, all β3GnTs are expressed within the first 24 hours of development and yet knockdown of several β3GnT

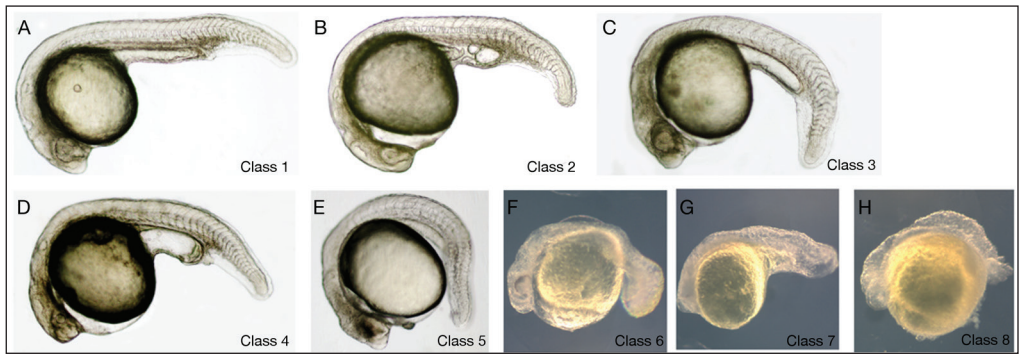

Figure 3. Knockdown of β3GnT expression results diverse patterning defects and reveals synergistic activity between various β3GnT genes. Embryos 24 hpi injected with morpholinos targeting a single β3GnT genes or combinations of multiple β3GnT genes shows an array of phenotypes that can be sorted into phenotypic classes. Defects can be seen in CNS and trunk mesenchyme patterning when only single β3GnT genes are knocked-down (B, C and E). Co-injection of multiple morpholinos reveals both redundant and synergistic effects resulting in a continued spectrum of CNS and mesenchyme patterning defects. Simultaneous knockdown of all β3GnT family members (H) results in severe patterning defects throughout the embryo. A summary of injection treatments and phenotypic classes can be found in Tables 2-4.

transcripts failed to produce a phenotype suggesting that these genes are not essential for early embryonic development. β3GnT5, in particular, did not show localized expression until the long-pec stage consistent with the lack of an early embryonic phenotype.

Since there is considerable sequence similarity and overlapping expression among the β3GnT genes, we wanted to determine if there was any redundancy between the different β3GnT genes. To accomplish this, we co-injected two different β3GnTMOs, keeping the total amount of injected MO to 10 ng, results summarizing these co-injections can be found in Table 3. Co-injection of β3GnT2b and β3GnT7b, two morpholinos that individually failed to result in any developmental defect, produced embryos with moderate CNS and trunk defects and were classified as Class 4 embryos (Fig. 3D). This result demonstrates that β3GnT2b and β3GnT7b do have essential functions during development; however, these functions are redundant and can be compensated by other glycosyltransferases. Furthermore, this double knockdown phenotype reinforces the finding that β3GnTs are involved in

Table 2. Knockdown of individual β3GnT transcripts.

Single β3GnT transcript knockdown	Total embryos injected	Total embryos displaying major phenotype (% of total)	Major phenotypic class observed (See Fig. 3)
GnT2a	163	129 (79%)	Class 2 (Fig. 3B)
GnT2b	117	117 (100%)	Class 1 (Fig. 3A)
GnT3	308	219 (71%)	Class 3 (Fig. 3C)
GnT5	122	122 (100%)	1
GnT7a	194	177 (91%)	Class 5 (Fig. 3E)
GnT7b	145	145 (100%)	1
GnT2a Mismatch	97	82 (85%)	1
GnT2a + mRNA	88	65 (74%)	1 (Fig. 4B)

Table 3. Double knockdown of two β3GnT transcripts.

Double β3GnT transcript knockdown	Total embryos injected	Total embryos displaying major phenotype (% of total)	Major phenotypic class observed (See Fig. 3)
GnT2a/GnT2b	89	69 (78%)	Class 6 (Fig. 3F)
GnT2a/GnT3	118	97 (82%)	3
GnT2a/GnT5	110	89 (81%)	2
GnT2a/GnT7a	114	81 (71%)	5
GnT2a/GnT7b	105	74 (70%)	Class 7 (Fig. 3G)
GnT2b/GnT3	96	83 (86%)	6
GnT2b/GnT5	71	58 (81%)	1
GnT2b/GnT7a	77	59 (76%)	Class 4 (Fig. 3D)
GnT2b/GnT7b	104	94 (90%)	4
GnT3/GnT5	93	89 (96%)	3
GnT3/GnT7a	85	66 (78%)	7
GnT3/GnT7b	112	105 (94%)	3
GnT5/GnT7a	87	78 (89%)	5
GnT5/GnT7b	92	85 (92%)	1
GnT7a/GnT7b	81	69 (85%)	7

patterning of the CNS and trunk mesoderm. Additional pairs of β3GnT knockdowns further demonstrated the synergism within the family: co-injection of β3GnT2a and β3GnT2b (Fig. 3F) resulted in embryos with mild CNS defects and severe trunk defects (Class 6) even though β3GnT2bMO alone did not have a phenotype. Similarly, co-injection of β3GnT7a and β3GnT7b (Fig. 3G) resulted in embryos with severe CNS and trunk defects. Not every pair of β3GnT transcripts demonstrated synergism, as co-injection of β3GnT2b and β3GnT5 resulted in Class 1 embryos (Table 3 and 4). The complexity of the synergistic interactions between β3GnT family members could be the result of differing levels of expression of the transferases involved, such as if one β3GnT transcript is expressed at much higher levels knockdown of this transcript is likely to result in a developmental defect (spatial dominance). Alternatively, the failure of two β3GnTs to interact may be due to discrete substrate specificity or localization for the particular β3GnTs. By design, the concentration of morpholino used remained constant throughout all experiments allowing the double transcript injections serve as an important internal control for morpholino specificity. If the phenotypes reported were due to morpholino toxicity we would expect the double injections to have a reduced phenotype when compared to the single transcript injections. Since the total morpholino injected remained constant, the functional concentration of each individual morpholino was reduced by half. In fact, we typically observed a more severe phenotype when two morpholinos were injected, a trend that continued when we injected morpholinos targeting three, four, five or all six family members, demonstrating that the phenotypes we are reporting are in fact specific for the β3GnT transcript targeted.

We continued to investigate the functional relationships between β3GnT transcripts by performing co-injections using MOs targeting three β3GnT transcripts (Table 4) as well as co-injections targeting every zebrafish β3GnT (Fig. 3H). These experiments resulted in embryos with profound patterning defects throughout the organism as predicted by the widespread expression of β3GnT transcripts. Even though the defects were widespread in these multiple gene knockdowns, the essence of the phenotypes was consistent with what we observed for the single and double β3GnT knockdowns - specifically, defects centered around abnormal CNS and trunk mesenchyme development. It is important to note that the total concentration of morpholino was the same in the multiple transcript knockdown ex-

Table 4. Knockdown of multiple β3GnT transcripts.

Triple and whole family β3GnT transcript knockdown	Total embryos injected	Total embryos displaying major phenotype (% of total)	Major phenotypic class observed (See Fig. 3)
GnT2a+2b+3	118	91 (77%)	6
GnT2a+2b+7b	74	69 (93%)	6
GnT2a+3+7a	128	91 (71%)	7
GnT2a+3+7b	108	79 (73%)	7
GnT2a+5+7a	74	56 (76%)	5
GnT2a+7a+7b	87	81 (93%)	5
GnT2b+3+7a	106	87 (82%)	6
GnT2b+3+7b	109	80 (75%)	6
GnT2b+5+7b	70	64 (92%)	4
GnT2b+7a+7b	73	66 (90%)	5
GnT3+7a+7b	72	57 (80%)	3
Whole β3GnT family	63	60 (95%)	Class 8 (Fig. 3H)

periments as in the single morpholino injections, and therefore, the increase in phenotypic severity can be attributed to the loss of enzymatic activity and not to morpholino toxicity.

To control for morpholino specificity, "rescue" experiments were performed by co-injecting gene specific morpholinos along with mRNA encoding the targeted transcript in which the morpholino site was mutated using silent mutations. Co-injection of the mRNA restored the wild-type phenotype demonstrating the specificity of the morpholino (Fig. 4A). To further control for the specificity of knockdown, the carbohydrate profile of control-injected embryos and embryos injected with morpholinos targeting all β3GnT genes was assayed using the *Lycopersicon esculentum* agglutinin lectin (LEA). LEA is a carbohydrate binding lectin which preferentially recognizes GlcNAc residues in b1,3 linkages. The LEA lectin is useful in this instance as the β3GnT family, by definition, generates b1,3 GlcNAc linkages. Whole mount lectin staining control injected (Fig. 4B) embryos showed LEA reactivity and thus GlcNAc residues in the eye, hindbrain ventricle, otic vesicle, pronephros and intersomitic tissues. LEA staining was almost completely lost in embryos injected with morpholinos targeting the whole β3GnT family (Fig. 4C). Carbohydrates were isolated from either control or β3GnT family-injected embryos and used as input for a blot to assay the carbohydrate content in both groups (Fig. 4D). 14 prominent GlcNAc-containing bands were absent when compared to equivalent staged control-injected embryos (arrows) The reactivity of LEA demonstrates that the knockdown of β3GnT transcripts affects overall protein glycosylation in a GlcNAc-dependent mechanism, as expected. It also highlights the heterogeneity of glycosylation targets for β3GnTs in the zebrafish embryo.

Shh signaling in the midbrain requires β3GnT2a activity

Even though β3GnT2a had uniform expression in 14-somite embryos, by 26-somites there was a distinct increase of expression in the midbrain/hindbrain boundary and in the

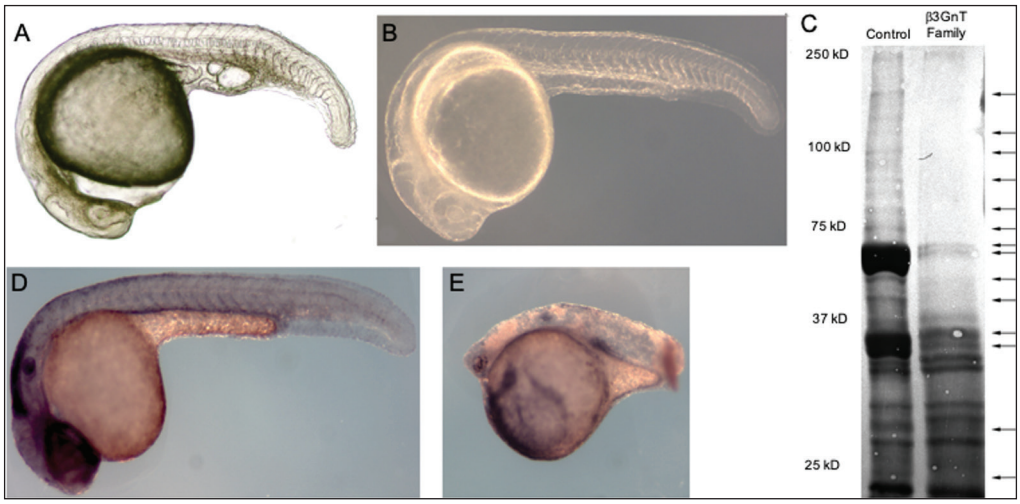

Figure 4. β3GnT morpholinos are specific for the targeted gene and result in reduced GlcNAc residues. (A) Injection of β3GnT2a as an example of one morphant phenotype, (B) dual injection of β3GnT2a morpholino and 40pg of β3GnT2a mRNA rescues the morphant phenotype. (C) Lectin blot utilizing LEA to detect GlcNAc residues in control- injected or β3GnT family-injected embryo lysate. Arrows highlight absent or reduced glycosylation in β3GnT-injected embryos. Embryos injected with either control or morpholinos targeting the whole β3GnT family were stained with LEA and reactivity was detected with BCIP/NBT. Control-injected embryos (D) show LEA reactivity in the eye, hindbrain, ventricles, otic vesicle, pronephros and intersomitic tissue. LEA reactivity is significantly reduced in the β3GnT family knockdown embryos (E).

pronephros. Consistent with this, knockdown of β3GnT2a produced embryos with defective midbrain and hindbrain structures in addition to the presence of globular structures in the yolk. To further characterize the defects produced by knockdown of β3GnT2a, *in situ* hybridizations were performed for markers expressed in the hindbrain/midbrain and in the trunk. In control-injected embryos, Islet-1 (*isl1*) is expressed diffusely throughout the hindbrain (asterisk in Fig. 5A) and in motor neurons of the trunk (arrowheads in Fig. 5A). In β3GnT2aMO-injected embryos, *isl1* continues to be expressed in the hindbrain, however the expression domain is compressed into a ventral region of the hindbrain (arrow in Fig. 5A). Furthermore, the *isl1* positive motor neurons in β3GnT2aMO-injected embryos are mis-localized along the dorsal-ventral axis of the trunk (arrowheads in Fig. 5A). Morpholino concentrations from 1 ng to 15 ng all resulted in the same *isl1* disruption, (data not shown) even though the severity of the phenotype increased. The disorganization of the trunk motor neurons may be a consequence of the underlying defects in mesenchyme morphology. Our previous studies have shown an involvement of fucosylation in the regulation of CNS development in a sonic hedgehog (*shh*) dependent manner, and as we observed defects in development of the CNS in β3GnT2aMO-injected embryos, further analysis was conducted on the hindbrain phenotype.

During zebrafish development, patterning of the midbrain and hindbrain boundary, which in turn directly impacts hindbrain structure, is controlled by a structure called the

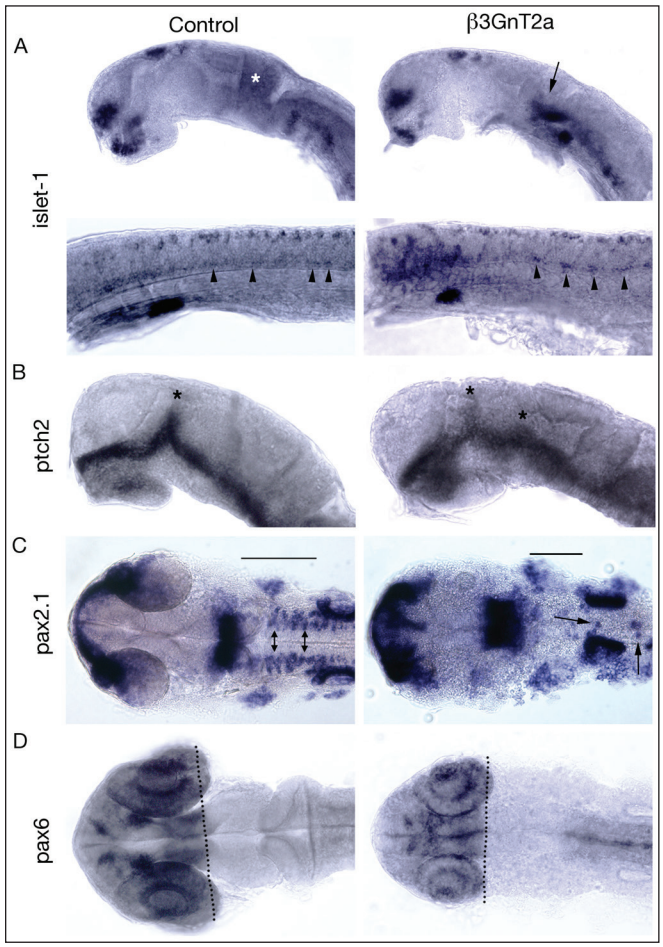

Figure 5. Knockdown of β3GnT2a effects *shh* signaling and disrupts hindbrain patterning. Control and β3GnT2aMO embryos at 26 hpi. *In situ* hybridization for *isl1* shows abnormal pattering of hindbrain (asterisk and arrow in A) and a disorganized distribution of motor neurons in the trunk (arrowheads in A'). *ptch2* (B) shows an elongation of the expression domain posterior to the ZLI in β3GnT2aMO embryos. As a consequence, the hindbrain domain of β3GnT2aMO embryos is smaller (denoted by bars in C) and formation of the hindbrain neurons is disrupted (arrows in C). *The pax6* expression domain in β3GnT2aMO embryos is unaffected (dashed line in D).

zona limitans intrathalamica (ZLI). The position of the ZLI is primarily determined by *shh* signaling (Scholpp et al. 2006). To investigate the effects of *shh* signaling in β3GnT2aMO injected embryos, we assayed the expression of Patched-2 (*ptch2*), a major signaling receptor for *shh* in the ZLI. Control-injected embryos express *ptch2* in the posterior forebrain with a characteristic peak in the ZLI (asterisk in Fig. 5B). β3GnT2aMO-injected embryos also express *ptch2* in a forebrain peak (paired asterisk in Fig. 5B), however the peak in the ZLI is elongated posteriorly, which we propose results in an abnormal ZLI. The abnormal ZLI presumably leads to an expanded midbrain/hindbrain domain, which effectively reduces the hindbrain. The reduced hindbrain domain was confirmed by *pax2.1* expression in β3GnT2aMO-injected embryos (bars in Fig. 5C). We also noticed a significant reduction and mis-localization of *pax2.1*-positive hindbrain neurons (arrows in Fig. 5C). We suggest that the effects on altered *pax2.1* expression are due to abnormal hindbrain pattering in response to the defective ZLI. If *pax2.1* activity was directly affecting the hindbrain phenotype, we would have expected to see an altered *pax6* expression, which was not observed in β3GnT2aMO-injected embryos (Fig. 5D). We have previously reported that *shh* signaling in the CNS is reduced in response to α1,6-fucosyltransferase 8 (FucT8) knockdown (Seth et al. 2010). Knockdown of FucT8 alters the glycosylation pattern of Apolipoprotein B100 (ApoB), a known transporter of *shh*. It is possible that β3GnT2a generates an epitope on ApoB that either is essential for *shh* binding or is further fucosylated and then interacts with *shh*.

Abnormal ganglion cell contribution in β3GnT5 morpholino-injected embryos

The expression pattern of β3GnT5 showed the greatest spatial and temporal specificity by being restricted to the lens of Prim-16 embryos and beyond, suggesting an essential function in the development of that organ. To test this hypothesis, we examined late-stage β3GnT5MO-injected embryos for defects in eye development. Interestingly, on a gross morphological level, embryos injected with a β3GnT5MO were phenotypically indistinguishable from control-injected embryos. To determine if any defects in the patterning of the retina occurred following injection, we performed a histological analysis of β3GnT5MO-injected and control-injected embryos. Hematoxylin and eosin stained thin sections of the eye confirmed that there was no dramatic alteration to the overall structure of the retina; however, there was a suggestion that the ganglion cell layer in the retina was altered in β3GnT5MO- injected embryos (Fig. 6B,C). To explore this possibility, we measured the relative size of each cell layer in control (blue bars in Fig. 6A) and β3GnT5MO-injected embryos (green bars in Fig. 6A). There was a small, but statistically significant ($P < 0.005$), increase in the proportion of cells in the ganglion cell layer (asterisk in Fig. 6A) and in the inner plexiform layer ($P < 0.01$) (double asterisk in Fig. 6A); all other layers of the retina were unaffected. These findings suggest that β3GnT5 expression in the lens is able to influence the number of ganglion cells produced in the zebrafish retina.

Discussion

β1,3-*N*-acetylglucosaminyltransferases are a family of glycosyltransferases encoded for by six genes in the zebrafish. We have shown that these genes are expressed throughout the development of the zebrafish embryo, and knockdown of these genes affects the development of the CNS and trunk mesenchyme. We have also experimentally demonstrated the hypothesized functional synergism and redundancy between family members. Furthermore, we have shown that β3GnT2a is involved in a *shh* mediated regulation of the hindbrain domain and β3GnT5 is involved in the specification of retinal ganglion cells.

Since glycosyltransferases are essential enzymes for generating diverse carbohydrate epitopes, it was expected that many tissues would require and therefore express a diverse array of β3GnT genes. All of the zebrafish β3GnT genes maintained expression once they were detectable by PCR, suggesting they are, at least partially, housekeeping genes. Further supporting this hypothesis is the widespread and seemingly unrestricted expression of β3GnT2b, β3GnT3, β3GnT7a and β3GnT7b. Maternal loading of β3GnT2a into the oocyte suggests β3GnT2a may be required for processes prior to zygotic gene transcription. Moreover, since β3GnT2a was the only gene with expression detected in early development (prior to epiboly) it is possible that β3GnT2a is the primary poly-*N*-acetyllactosamine synthase in zebrafish. This activity is hypothesized for early development when β3GnT2a is the only β3GnT gene expressed. It is possible that poly-*N*-acetyllactosamine synthase activity is shared by redundant β3GnT genes later throughout embryonic development. The mammalian β3GnT2a homologue is the dominant poly-*N*-acetyllactosamine synthase in mammals, although the null mutant is embryonic viable suggesting redundant enzymatic functions within the protein family. Interestingly, β3GnT2a is also one of the few β3GnT transcripts to show localized expression later during development. The increased expression in the CNS as well as in the pronephros could indicate a specific requirement for β3GnT2a activity in those tissues. The only other transcript to show tissue-specific expression is β3GnT5, which is expressed exclusively during later development of the lens. While the

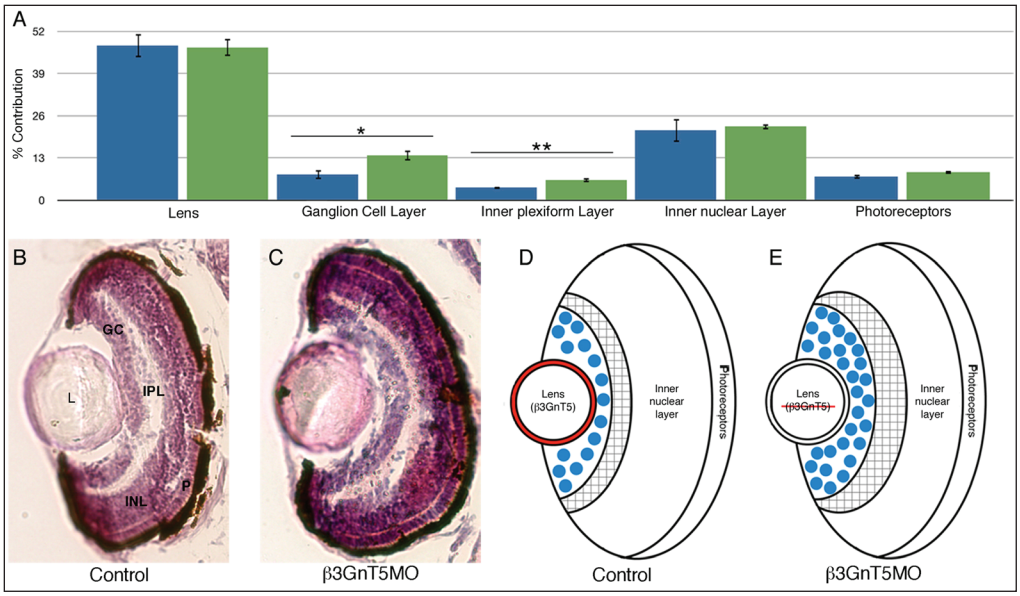

Figure 6. Knockdown of β3GnT5 increases the ganglion cell and inner plexiform layers of the retina. Quantitative analysis of each retinal cell layer shows that each layer is altered in β3GnT5MO embryos (green in A) as compared to control-injected embryos (blue in A). β3GnT5MO embryos had a significantly larger ganglion cell layer (asterisk in A), and inner plexiform layer (double asterisk in A), while the lens, inner nuclear layer and photoreceptors were unaffected. (B and C) H+E sections of control or β3GnT5MO eyes at 48 hpi. A model representing β3GnT5 activity, where β3GnT5 is expressed in the wild-type lens (D) and produces carbohydrate epitopes that are expressed on the cell surface (red). Knockdown embryos (E) do not expresses β3GnT5 in the lens, thereby producing an altered cell surface epitope. The adjacent ganglion cells begin to occupy a greater domain, which we hypothesize is due to proliferation (blue circles) and thus require additional area to synapse, thus the expanded inner plexiform layer (grey hash). L (Lens), GC (ganglion cells), IPL (inner plexiform layer), INL (inner nuclear layer), P (photoreceptors).

function of β3GnT5 generated epitopes in the lens was unclear, Nakayama and colleagues has shown that β3GnT5 expression in the lens requires fgf19 activity, as knockdown of fgf19 eliminated β3GnT5 expression (Nakayama et al. 2008).

To investigate the function of β3GnTs during zebrafish development we systematically knocked-down the expression of all β3GnT transcripts, either individually or in various combinations of multiple transcripts. Following morpholino knockdown, we determined that β3GnT activity is required for many aspects of vertebrate development but particularly restricted to pattern formation of the trunk mesenchyme and pattering of the CNS. Since β3GnT polypeptides are restricted to the Golgi complex, the developmental effects of these enzymes must be derived from the carbohydrate epitopes expressed on membrane bound, and possibly secreted, glycoconjugates. We showed that by LEA reactivity of β3GnT family-injected embryos that at least 14 different glycoconjugates are affected, any of which could be responsible for the manifestation of the CNS and mesenchyme phenotype. Although well beyond the scope of this study, identifying the substrates that are glycosylated by the individual β3GnT enzymes would allow us to further dissect the mechanisms by which these complex carbohydrates mediate developmental processes.

A fundamental complication encountered when investigating functional glycomics is the close enzymatic activity seen between members of the same family. *In vitro* studies have elucidated the catalytic activity of many β3GnT enzymes, yet little is known about the *in vivo* activity of these enzymes. We have demonstrated that there is functional synergism between members of the β3GnT family as well as functional redundancy between members of the β3GnT family. For our investigation we have defined synergism as the ability of two proteins that each produce a knockdown phenotype to produce a third more complex phenotype when knocked-down in the same embryos, as seen by co-injection of β3GnT2a and β3GnT7a (Fig. 3E). Synergism is distinct from redundancy in that redundant proteins do not result in a phenotype when individually knocked-down, only when both transcripts are targeted in the same embryo is a phenotype observed, as seen by co-injection of β3GnT2b and β3GnT7b (Fig. 3D). Further tests into the mechanism of the synergistic versus redundant activity could include rescuing morpholino produced phenotypes with mRNAs predicted to have synergistic activity. For example; as β3GnT2b and β3GnT7b are functionally redundant, then the β3GnT2b mRNA would be predicted to rescue, or partially rescue, the double knockdown phenotype.

Even though we report functional synergism within the β3GnT family, we were able to identify discrete functions for two individual transferases. β3GnT2a had increased expression in the midbrain/hindbrain boundary by the 26-somite stage, and transcript specific knockdown resulted in Class 2 embryos. The mild phenotype observed was mostly restricted to the developing CNS, and closer analysis revealed that the hindbrain domain of β3GnT2aMO-injected embryos was abnormally patterned. We determined that this phenotype is due to abnormal *shh* expression in the ZLI. The position of the ZLI in zebrafish is determined by a *shh* gradient and then the ZLI itself is responsible for further pattering of the midbrain and the hindbrain (Scholpp et al. 2006). In β3GnT2aMOs the *shh* expression domain is expanded posteriorly, causing a posterior shift in the ZLI and ultimately altering the hindbrain pattern. We have shown previously that knockdown of FucT8 can alter *shh* signaling by reducing *shh*-ApoB binding (Seth et al. 2010). It is possible that the loss of GlcNAc residues in β3GnT2aMO effectively eliminates fucose residues as well.

Numerous reports have investigated the glycoconjugate composition of the vertebrate lens, and while few glycoproteins have been identified, there is strong evidence to suggest

that the surface of the lens is covered with a mosaic of glycoconjugates and proteoglycans (Yao et al. 1996). One of the dominant glycosidic moieties found in the eye of vertebrates in sulfated keratin sulfate (Conrad and Conrad 2003). Keratin sulfate is decorated with sulfated polylactosamine, which requires β3GnT activity for synthesis (Togayachi et al. 2010). Here we show that β3GnT5 is expressed specifically in the developing lens, and by using morpholino knockdown, we show that eyes of β3GnT5-morpholino injected embryos have an abnormal composition of cells.

A recent study has shown that sulfated proteoglycans inhibit neurite growth in retinal ganglion cells and furthermore, blocking these proteoglycans can stimulate neurite growth (Brown et al. 2012). It is possible that β3GnT5 participates in the generation of these proteoglycans and the knockdown of β3GnT5 mimics the blockage and facilitates neurite growth. Knockdown of FucT8 also affects the development of the zebrafish eye, however FucT8 affects the early differentiation of retinal cells, and is not a specific effect on ganglion cells so it is unlikely that the mechanisms regulating β3GnT2 and β3GnT5 activity are the same (Seth et al. 2010). Most eye patterning defects reduce the overall size of the eye, so it is interesting that we do not observe this in β3GnT5MO-injected embryos, nor do we observe an overall increased in the size of the eye to accommodate the increase in the proportion of ganglion cells. It is possible that this modulation of eye size is due to an insignificant reduction in other cell layers, or to an insignificant increase in the overall size of the eye, neither of which we were able to detect.

Based on these data and our understanding of β3GnT catalytic activity, we present a simple working model to account for some of the β3GnT5MO effects (Fig. 6D,E). We postulate that GlcNAc residues are tethered to the lens surface where they preferentially interact with cells in the ganglion layer and regulate their overall proliferation. Following injection of β3GnT5MO, the expression of GlcNAc residues on lens surface glycoproteins are reduced, leading to an increase in the number of retinal ganglion cells or to an increase in the overall size of the dendridic arbor of the ganglion cells, which would require a proportional increase in the number of synapses with amacrine, horizontal and bipolar cells within the inner plexiform layer (IPL). If our model is accurate, we would not expect to observe significant changes to the overall rate of proliferation or a decrease in apoptosis as we propose the presence of β3GnT5 influences the available space for the ganglion cells to occupy.

In summary, we report here the characterization of a family of β1,3-*N*-acetylglucosaminyltransferases in zebrafish that has diverse functions, particularly within the development of the CNS and trunk mesenchyme. Using molecular phylogenetic analysis, we refined the classification of six zebrafish β3GnTs as a family distinct from the closely related β3GalT family and the enzymatically similar *lfng* family. All β3GnT genes are expressed by the 1-somite stage and their expression remains detectable throughout embryonic development. β3GnT2a and β3GnT5 shows refined expression within the CNS and lens, respectively, while all other β3GnTs have widespread expression patterns. Knockdown of individual β3GnT genes results in a spectrum of CNS and trunk mesenchyme patterning defects, and co-injection of multiple β3GnTs reveals functional synergisms between family members. Further analysis of the β3GnT2a knockdown phenotype demonstrates involvement in *shh*-mediated hindbrain patterning, while β3GnT5 is involved in the regulation of ganglion cells in the retina. Additional studies are required to further define the mechanisms by which these genes, and their glycoconjugate substrates, function during embryonic development.

Acknowledgements

This work was partially supported by NIH grant [DE17120] to BDS and AF. Additional support was provided by Manhattan College as awarded to QJM.

Literature Cited

Bao, X., M. Kobayashi, S. Hatakeyama, K. Angata, D. Gullberg, J. Nakayama, M.N. Fukuda, and M. Fukuda. 2009. Tumor suppressor function of laminin-binding alpha-dystroglycan requires a distinct beta3-N-acetylglucosaminyltransferase. Proceedings of the National Academy of Sciences USA 106:12109–12114.

Biellmann, F., T.R. Henion, and K. Burki, and T. Hennet. 2008a. Impaired sexual behavior in male mice deficient for the beta1-3 N-acetylglucosaminyltransferase-I gene. Molecular Reproduction and Development 75:699–706.

Biellmann, F., A.J. Hulsmeier, D. Zhou, P. Cinelli, and T. Hennet. 2008b. The Lc3-synthase gene B3gnt5 is essential to pre-implantation development of the murine embryo. BMC Developmental Biology 8:109.

Brown, J.M., J. Xia, B. Zhuang, K.S. Cho, C.J. Rogers, C.I. Gama, M. Rawat, S.E. Tully, N. Uetani, and D.E. Mason. 2012. A sulfated carbohydrate epitope inhibits axon regeneration after injury. Proceedings of the National Academy of Sciences USA 109:4768–4773.

Chou, C.M., J.H. Leu, and C.J. Huang. 2000. A family of novel genes encoding beta-3-galactosyltransferase from zebrafish. Taipei: Institute of Biological Chemistry, Academia Sinica.

Colley, K.J. 1997. Golgi localization of glycosyltransferases: More questions than answers. Glycobiology 7:1–13.

Conrad, A.H., and G.W. Conrad. 2003. The keratocan gene is expressed in both ocular and non-ocular tissues during early chick development. Matrix Biology 22:323–337.

Dunwoodie, S.L. 2009. Mutations of the fucose-specific beta1,3 N-acetylglucosaminyltransferase LFNG results in abnormal formation of the spine. Biochimica et Biophysica Acta 1792:100–111.

Hayashi, N., S. Nakamori, J. Okami, H. Nagano, K. Dono, K. Umeshita, M. Sakon, H. Narimatsu, and M. Monden. 2004. Association between expression levels of CA 19–9 and N-acetylglucosamine-beta:1,3 galactosyltransferase 5 gene in Human pancreatic cancer tissue. Pathobiology 71:26–34.

Johnston, S.H., C. Rauskolb, R. Wilson, B. Prabhakaran, K.D. Irvine, and T.F. Vogt. 1997. A family of mammalian Fringe genes implicated in boundary determination and the Notch pathway. Development 124:2245–2254.

Kanie, O., S.C. Crawley, M.M. Palcic, and O. Hindsgaul. 1993. Acceptor-substrate recognition by N-acetylglucosaminyltransferase-V: critical role of the 4'-hydroxyl group in beta-D-GlcpNAc-(1→2)-alpha-D-Manp(1→6)-beta-D-Glcp-OR. Carbohydrate Research 243:139–164.

Kimmel, C.B., W.W. Ballard, S.R. Kimmel, B. Ullmann, and T.F. Schilling. 1995. Stages of embryonic development of the zebrafish. Developmental Dynamics 203:253–310.

Knott, T.K., P.A. Madany, A.A. Faden, M. Xu, J. Strotmann, T.R. Henion, and G.A. Schwarting. 2012. Olfactory discrimination largely persists in mice with defects in odorant receptor expression and axon guidance. Neural Development 7:17.

Kuan, C.T., J. Chang, J.E. Mansson, J. Li, C. Pegram, P. Fredman, R.E. McLendon, and D.D. Bigner. 2010. Multiple phenotypic changes in mice after knockout of the B3gnt5 gene, encoding Lc3 synthase: A key enzyme in lacto-neolacto ganglioside synthesis. BMC Developmental Biology 10:114.

Nakayama, Y., A. Miyake, Y. Nakagawa, T. Mido, M. Yoshikawa, and M. Konishi, and N. Itoh. 2008. GFG19 is required for zebrafish lens and retina development. Developmental Biology 313:752–766.

Rampal, R., A.S. Li, D.J. Moloney, S.A. Georgiou, K.B. Luther, A. Nita-Lazar, and R.S. Haltiwanger. 2005. Lunatic fringe, manic fringe, and radical fringe recognize similar specificity determinants in O-fucosylated epidermal growth factor-like repeats. Journal of Biological Chemistry 280:42454–42463.

Scholpp, S., O. Wolf, M. Brand, and A. Lumsden. 2006. Hedgehog signaling from the zona limitans intrathalamica orchestrates patterning of the zebrafish diencephalon. Development 133:855–864.

Seth, A., Q.J. Machingo, A. Fritz, and B.D. Shur. 2010. Core fucosylation is required for midline pattering during zebrafish development. Developmental Dynamics 239:3380–3390.

Shiraishi, N., A. Natsume, A. Togayachi, T. Endo, T. Akashima, Y. Yamada, N. Imai, S. Nakagawa, and S. Koizumi, and S. Sekine. 2001. Identification and characterization of three novel beta1,3-N-acetylglucosaminyltransferases structurally related to the beta 1,3-galactosyltransferase family. Journal of Biological Chemistry 276:3498–3507.

Thisse, C., and B. Thisse. 2008. High-resolution in situ hybridization to whole-mount zebrafish embryos. Nature Protocols 1:59–69.

Togayachi, A., Y. Kozono, A. Kuno, T. Ohkura, T. Sato, J. Hirabayashi, Y. Ikehara, and H. Narimatsu. 2010. Beta3GnT2 (B3GNT2), an major polylactosamine synthase: Analysis of B3GNT2-deficient mice. Methods in Enzymology 479:185–204.

Varki, A. 1993. Biological roles of oligosaccharides: All of the theories are correct. Glycobiology 3:97–130.

Westerfield, M. 2000. The zebrafish book. A guide for the laboratory use of zebrafish (*Danio rerio*). 4th edition. University of Oregon Press. Eugene, OR.

Yamamoto, F., H. Clausen, T. White, J. Marken, and S. Hakomori. 1990. Molecular genetic basis of the histo-blood group ABO system. Nature 345:229–233.

Yao, R., W. Crossland, and H. Maisel. 1996. Electron microscopic detection of glycoconjugates in the chicken lens. Experimental Eye Research 63:705–711.

Zhou, D., A. Dinter, R. Gutierrez Gallego, J.P. Kamerling, J.F. Vliegenthart, E.G. Berger, and T. Hennet. 1999. A beta-1,3-N-acetylglucosaminyltransferase with poly-N-acetyllactosamine synthase activity is structurally related to beta-1,3-glactosyltransferase. Proceedings of the National Academy of Sciences USA 96:406–411.